



Least fractional order memristor nonlinearity to exhibits chaos in a hidden hyperchaotic system

S. Sabarathinam¹ · D. Aravinthan² · Viktor Papov¹ · R. Vadivel³ · N. Gunasekaran⁴

Received: 25 January 2023 / Revised: 28 June 2024 / Accepted: 27 July 2024 /
Published online: 5 August 2024
© Diogenes Co.Ltd 2024

Abstract

In this article, we present least fractional nonlinearity for exhibiting chaos in a memristor-based hyper-chaotic multi-stable hidden system. When implementing memristor-based systems, distinct dimensions/order define the memristor nonlinearity. In this work, the memristor dimension has been changed fractionally to identify the lowest order of nonlinearity required to induce chaos in a proposed system. The two-parameter frequency scanning helps in understanding both oscillation and non-oscillation regimes. The system fractional nonlinearity strength will help in deeper understanding of mathematical modelling and control. In addition, multistability and hidden oscillations were thoroughly investigated in the proposed system. The current work combines analytical, numerical, and experimental methods to demonstrate the system dynamics.

✉ S. Sabarathinam
saba.cnld@gmail.com

D. Aravinthan
d.aravinthan@gmail.com

Viktor Papov
masterlu@mail.ru

R. Vadivel
vadivelsr@yahoo.com

N. Gunasekaran
gunasmaths@gmail.com

- ¹ Laboratory of Complex Systems Modelling and Control, Faculty of Computer Science, National Research University, HSE, Moscow, Russia
- ² Department of Sciences, Mathematics and Education, St. Joseph College of Engineering and Technology, St. Joseph University, 11007 Dar es Salaam, Tanzania
- ³ Department of Mathematics, Phuket Rajabhat University, Phuket 83000, Thailand
- ⁴ Department of Natural Sciences, Eastern Michigan Joint College of Engineering, Beibu Gulf University, Qinzhou 535 011, China

Keywords Memristor emulator · Fractional order memristor · Multistability · Least order memristor · Hidden attractor

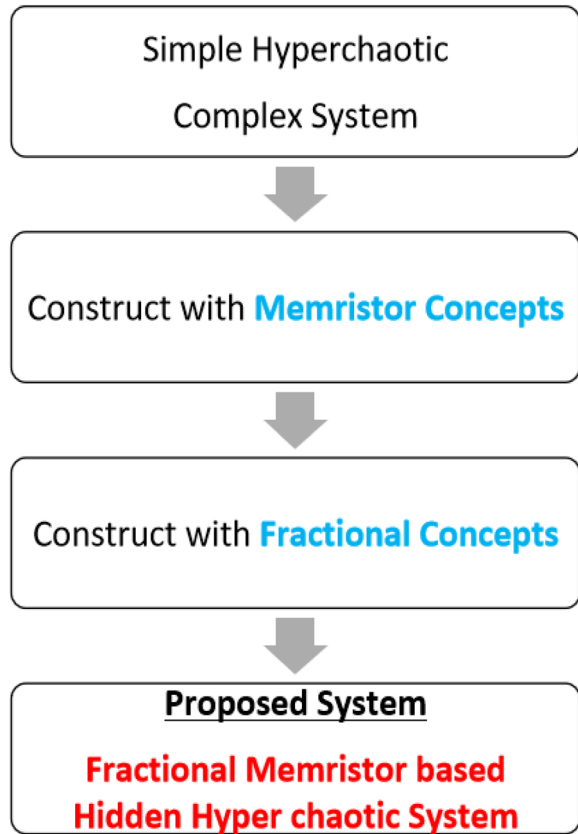
1 Introduction

Recently, it has been discovered that a rising number of physical systems are best characterised by fractional order differential equations rather than traditional integer order equations. In particular mass diffusion, heat conduction processes, distributed lines, electrochemical processes, dielectric polarisation, viscoelastic materials like polymers and rubbers, relaxation phenomena of organic dielectric materials, flexible structures, traffic in information networks, and biological systems [29, 32, 38, 48]. As a result, the scientific community is becoming increasingly interested in identifying fractional order systems. However, these models present a more complex identification challenge, necessitating not only the estimate of model coefficients but also the determination of fractional orders via the time-consuming calculation of fractional order derivatives. Despite the loss of integer order, which complicates the identification process, certain identification approaches for fractional order systems in the frequency and time domains have been presented [27].

Moreover, there has been an increasing interest in fractional order complex systems, notably memristor-based fractional order systems, which have revealed various hitherto undiscovered dynamics [3, 20, 39]. The fractional order idea connects the mathematical tool of fractional calculus with the mathematical branch of chaos theory. Munoz et al. discovered multiple hidden attractors in the basin of a fractional order chaotic system using frac-memristors [23]. Prakash et al. [31] studied fractional order backstepping control using a memristor-based chaotic jerk system. All studies on dynamical systems focus on understanding their dynamics and stability by altering the state variable ordering as fractions [14, 22, 28].

On the other hand, in recent years, many articles on hidden complex systems addressed the key characteristics of the hidden dynamics [19]. Hidden attractors have been discovered in numerous natural and biological systems. Hidden characteristics in complex systems can be found in isolated and coupled configurations of Chua, Lorenz, Roseller, Sprott oscillators, etc. [15, 48, 49]. These studies are extremely useful in identifying and understanding various types of stability, attractors, and so on. Even though the mechanism and justification for such hidden attractors are still unclear in general. However, there are few studies in the literature on the reasons and methods behind the hidden dynamics [42]. Several articles in various domains have reported on the memristor-based hidden attractor [1, 9, 10, 17, 21, 36, 37, 40, 50]. Wang et al. found hidden and coexisting attractors in a modified Chua's circuit [46] and Sprott-A system with perpetual points [47]. Chen et al. reported the memristor-based Chua circuit and studied both self-excited and hidden dynamics [8]. Pham et al. reported hidden attractors in the memristor-based hyperchaotic system and report its synchronisation and circuit constructions [30]. Similarly, the multistability of hidden attractors was reported by Chang et al. [7] and Musha et al. [16]. The memristor conceptual, the boosting behaviour of hyperchaotic systems, was studied by Wu et al. [51]. Xu et al. examined multiple attractors in a memristor-based Chua circuit [54].

Fig. 1 A sketch of the current manuscript's workflow



Wang et al. investigate hidden dynamics, synchronisation, and circuit implementation of their article on fractional order memristor-based chaotic systems [45].

Furthermore, nonlinearity is very important for modelling, design, and structural analysis in many fields, from engineering to biological nonlinear models. It plays a key role in the system sensitivity, structural variations, and boundedness [35]. The nonlinearity plays a role in dynamical systems take place of phase shift, exponential grow or decay and chaotic. Additionally, experimental validation must be able to identify, characterise, and quantify nonlinearities. Assessing nonlinearities is another challenge since many nonlinear dynamical systems consist of more than one nonlinear components, which are difficult to calculate. However, in a memristor-based nonlinear system, the nonlinearity gets individual dimension/order. In this article, we propose a hidden hyperchaotic memristor system to determine the least-order nonlinearity strength for generating chaos. This manuscript addresses the subject, “*What is the minimum order of nonlinearity needed to achieve chaos?*” To the author’s knowledge, this is the first study of fractional nonlinearity in memristor-based hidden hyperchaotic dynamical systems. Figure 1 illustrates the study’s outline.

The manuscript is organised as follows: Section 2 describes the structure of fractional order derivatives as well as the formation of memristor-based systems. Section 3

shows how to build a fractional order hyperchaotic oscillator using memristors. The stability and multistability are performed in the same section. Section 4 discusses the numerical and experimental results. The two parameter scanning are also discussed in the same section. Finally, Section 5 summarises the results of the manuscript.

2 Fractional derivatives and integrals

Several definitions for fractional derivatives and integrals have been employed in recent years, for example, in works like [12, 41], see also some definitions in older source [25]. Riemann-Liouville (RL) fractional operator [27] and Caputo’s fractional operators [6] are commonly used by researchers to formulate fractional order systems. In this manuscript, we used the Riemann-Liouville (RL) fractional operator to construct the memristor-based fractional hyperchaotic system.

As for the RL operator, it meets the mathematical principle of fractional calculus. A new series formula, $D^q y(t)$, $0 < q < 1$ for approximating the fractional derivative operator in the sense of RL is presented in this manuscript. We derive this formula from the weighted mean value theorem (WMVT) and some direct computations. It is extremely difficult to find solutions to some linear and nonlinear fractional differential equations; this formula is very useful for establishing new approaches. In many cases, these series of solutions can be used to determine the analytic solutions.

2.1 Riemann–Liouville differential and integral operators

We remind the definitions and properties of these operators. Assuming $[A, B]$ is a finite interval, $-\infty < A < B < \infty$, the left-sided Riemann-Liouville (lsRL) integral of order $q \in R^+$ is defined:

$$K_{A^+}^q f(x) = \frac{1}{\Gamma(q)} \int_x^A \frac{f(\tau)}{(x - \tau)^{1-q}} d\tau, \quad x > A, \tag{1}$$

and the right-sided Riemann-Liouville (rsRL) fractional integral of order $q \in R^+$:

$$K_{B^-}^q f(x) = \frac{1}{\Gamma(q)} \int_x^B \frac{f(\tau)}{(\tau - x)^{1-q}} d\tau, \quad x < B. \tag{2}$$

We have confined the fractional order values to real positive numbers, which is needed for some practical applications, but one may find that q is a complex number [34]. The lsRL fractional derivative of order $q \in R^+$ is defined:

$$D_{A^+}^q f(x) = \frac{1}{\Gamma(n - q)} \frac{d^n}{dx^n} \int_x^A \frac{f(\tau)}{(x - \tau)^{q-n+1}} d\tau, \quad x > A, \tag{3}$$

and

$$D_A^q f(x) = \frac{1}{\Gamma(n - q)} \frac{d^n}{dx^n} \int_A^x \frac{f(\tau)}{(x - \tau)^{q-n+1}} d\tau, \quad x > A. \tag{6}$$

It should be mentioned that the integral operators $K_{A^+}^q$, $K_{B^-}^q$ and K_A^q in (1), (2), and (5), respectively, defined on the Laplace transform of $L^p(A, B) \equiv$ the space of integrable functions, where $p \in [1, \infty)$ [4]. Whereas the differential operators $D_{A^+}^q$, $D_{B^-}^q$, and D_A^q in (3), (4) and (6) respectively, are defined on $C[A, B] \equiv$ the space of continuous functions. Next, some important properties of the integral operator are stated for completeness.

1. Let $q, \beta \geq 0$ and $\phi \in L^1[A, B]$. Then $K_A^q, K_B^q \phi = K_A^{q+\beta} \phi$ holds almost everywhere on $[A, B]$. If additionally $\phi \in C[A, B]$ or $q + \beta \geq 1$, then the identity holds everywhere on $[A, B]$.
2. Let $q, \beta > 0$ and $\phi \in L^1[A, B]$. Then $K_A^q, K_B^q \phi = K_B^q K_A^\beta \phi$.
3. The RL fractional integral K_A^q of the power function satisfies,

$$K_A^q (x - A)^\mu = \frac{\Gamma(\mu + 1)}{\Gamma(\mu + q + 1)} (x - A)^{\mu+q}, \quad q > 0, \mu > -1. \tag{7}$$

Having mentioned some fundamental properties of RL integral operator, next we are ready to state some properties of the corresponding RL differential operator.

4. Let $q \geq 0$. Then for every $f \in L^1[A, B]$, we have $D_A^q, K_A^q f(x) = f(x)$, which exists almost everywhere [11].
5. Let $q \geq 0$, if there exists some $\phi \in L^1[A, B]$ such that $f = K_A^q \phi$, then, $D_A^q, K_A^q f(x) = f(x)$ almost everywhere [11].
6. Let $q > 0$ and $n - 1 \leq q < n, n \in \mathbb{N}$. Assume that f is such that $K_A^{(n-q)} f \in C^n[A, B] \equiv$ the set of all functions with an absolutely continuous $(n - 1)^{th}$ derivative [11], we get

$$D_A^q K_A^q f(x) = f(x) - \sum_{k=0}^{n-1} \frac{(x - A)^{q-k-1}}{\Gamma(q - k)} \lim_{z \rightarrow A^+} D^{(n-k-1)} K_A^{(n-q)} f(z). \tag{8}$$

In particular, for $0 < q < 1$, we have

$$D_A^q K_A^q f(x) = f(x) - \frac{(x - A)^{q-1}}{\Gamma(q)} \lim_{z \rightarrow A^+} K_A^{(1-q)} f(z). \tag{9}$$

7. Then the RL fractional derivatives D_A^q of the power function satisfy [11]:

$$D_A^q (x - A)^\mu = \frac{\Gamma(\mu + 1)}{\Gamma(\mu - 1 - q)} (x - A)^{\mu-q}, \text{ if } q - \mu \notin \mathbb{N}. \tag{10}$$

From (6), the Euler Gamma function is $\Gamma(\cdot)$ and considered by $(n - 1) \leq q < n$. At $t = 0$, all initial conditions are considered to be zero. Here, the Laplace transform of the RL fractional derivative can be written as,

$$L \left\{ \frac{d^q f(t)}{dt^q} \right\} = S^q L \{f(t)\}. \tag{11}$$

In the above, the order of the fractional derivative is described by ‘ q ’. The operator ‘ q ’ is a transfer function that is written in the *frequency domain*, i.e., $F(s) = \frac{1}{s^q}$. The definitions of fractional integrals do not allow for direct execution of the operator of complex systems with fractional elements in time-domain simulations. To investigate the system, the fractional operators should be approximated using standard integer-order operators. The linear transfer method for fractional integrator approximations of the order from 0.1 to 0.9, constructed using frequency domain statements, and the corresponding counterpart representations are presented in [2, 13, 44].

In experiments, the electronic circuit representative of tree shape circuit is shown in Figure 2(c), is developed to recognise the fractional order operator in [26, 52] by varying the resistance and capacitance values by adding new RC layers gives the changes in the fractional derivatives. Established with the fractional frequency-domain approximation $\frac{1}{s^q}$ can be modelled using a cascade of the tree shape model. One can obtain approximation of $\frac{1}{s^{0.9}}$ with an error of 2dB as follows: $\frac{1}{s^{0.9}} = \frac{2.2675(s+1.292)(s+215.4)}{(s+0.01292)(s+2.154)(s+359.4)}$. The values of the capacitors and resistors for obtaining the fractional order of $q_4 = 0.7$ are mentioned in Table 1. Figure 2(d) shows the experimentally observed $v - i$ characteristic of fractional order at (i) $q_4 = 0.99$, (ii) $q_4 = 0.7$, (iii) $q_4 = 0.4$ of the memristor emulator. The regime of the pinched hysteresis loop lowers as the fractional order of the memristor emulator is reduced, as seen in Figure 2. The external waveform generator was used to generate the $v - i$ characteristic curve, which had a amplitude of 2V and frequency of 1KHz.

2.2 Construction of memristor nonlinearity (cubic)

The memristor is defined by two types of nonlinear constitutive interactions between its voltage (v) and current (i):

$$\begin{cases} v = M(q)i, \\ i = W(\phi)v, \end{cases} \tag{12}$$

where $W(\phi)$ and $M(q)$ are nonlinear functions of flux (ϕ) and charge (q), which are called *memductance* and *memristance* [24] defined by:

$$\begin{cases} M(q) = \frac{d\phi(q)}{dq}, \\ W(\phi) = \frac{dq(\phi)}{d\phi}. \end{cases} \tag{13}$$

The memristor developed in this manuscript is a charge-controlled memristor, represented by the association in (12). The link between the terminal voltage and the

terminal current of the memristor is acquired by:

$$\begin{cases} v = \frac{d\phi}{dt} = \frac{d\phi}{dq} \frac{dq}{dt} = \frac{d\phi}{dq} i = M(q)i, \\ i = \frac{dq}{dt} = \frac{dq}{d\phi} \frac{d\phi}{dt} = \frac{dq}{d\phi} v = W(\phi)v. \end{cases} \tag{14}$$

The cubic nonlinearity is considered to transform as a memristor emulator and is defined as:

$$\begin{cases} \phi(q) = \xi q + \nu q^3, \\ q(\phi) = \xi \phi + \nu \phi^3. \end{cases} \tag{15}$$

The *memristance* and *memductance* is connected to flux and charge as:

$$\begin{cases} M(q) = \frac{d\phi}{dq} = \xi + 3\nu q^2, \\ W(\phi) = \frac{dq}{d\phi} = \xi + 3\nu \phi^2. \end{cases} \tag{16}$$

Notice that $M(q)$ and $W(\phi)$ are the *memristance* and *memductance* emulators [33]. The cubic nonlinearity is employed in this manuscript to create a memristor-based hidden hyperchaotic system.

3 Hidden hyperchaotic dynamical system

To begin, this section investigates the four-dimensional hyperchaotic memristor-based hidden system is under consideration and study the effect of fractional order nonlinearity [5]. The memristive hyperchaotic hidden system is described as follows:

$$\begin{cases} \frac{dx_1}{dt} = \epsilon W(x_4)x_2 - \eta x_1, \\ \frac{dx_2}{dt} = \gamma x_1 - x_1x_3 + \mu, \\ \frac{dx_3}{dt} = x_1x_2 - \zeta x_3, \\ \frac{dx_4}{dt} = x_2, \end{cases} \tag{17}$$

where $W(x_4) = \xi + 3\nu x_4^2$ is memristor (*memductance*) emulator. The state variable x_4 is considered flux ϕ . The parameter values of the system (17) are $\eta = 35, \zeta = 3, \gamma = 35, \epsilon = 40,$ and $\mu = 1$ and the nonlinearity coefficients are $\xi = 1, \nu = 0.02$ fixed throughout the manuscript. The initial conditions are fixed as $x_1(0), x_2(0), x_3(0),$ and $x_4(0) = (0.1, 0.1, 0, 0)$ for numerical results.

3.1 Hidden attractors and multistability

To calculate the stability of the system (17) by considering the derivatives are zero, the system has four equilibrium points, i.e. $x_1(0), x_2(0), x_3(0),$ and $x_4(0) = 0$. Further, eigenvalues are calculated in the trivial equilibrium point to identify the stability of the

Fig. 3 Numerically computed three-phase chaotic attractor in the x_1, x_2, x_3 plane of system (17) with fixed parameters. The trivial equilibrium of the system, S_0 is mentioned in the blue dot in the Figure

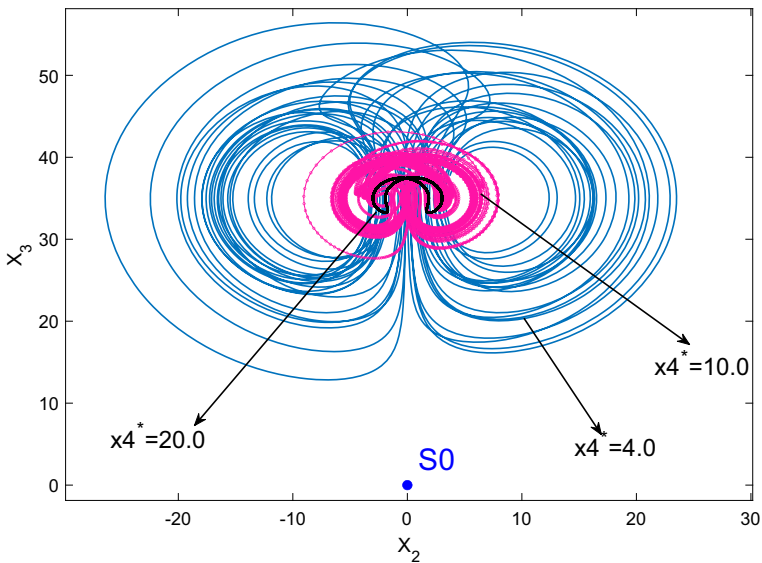
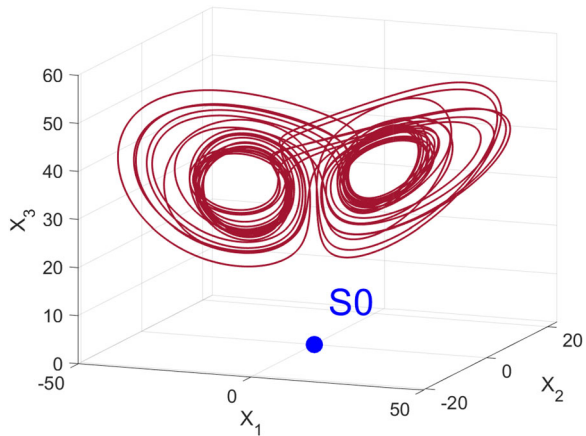


Fig. 4 Numerically computed multistability of system (17) with respect to the initial condition $x_4(0)$ and the rest IC's: $(x_1(0), x_2(0), x_3(0))$ are $(0.1, 0.1, 0.0)$. Chaotic (blue), periodic (black) attractor with different IC: $x_4(0)$

system. The eigenvalues are, $\lambda_1 = 0, \lambda_2 = 0.9730, \lambda_3 = -35.9730,$ and $\lambda_4 = -3.0000$. From this eigenvalues, the system has *saddle node* in its trivial equilibrium at zero.

From this stability, the system could not have attractor. But, far from the equilibrium, the system has chaotic oscillation, which is shown in Figure 3 in the three-dimensional visual and the trivial equilibrium point is mentioned as S_0 . The attractor is oscillating far from the origin never comes to an equilibrium, called as ‘*hidden attractor*’ [43].

Figure 4 shows the multistability of the system (17) with respect to the initial condition $x_4(0)$. The three colours represent the chaotic (blue) and periodic (black) attractors with different ICs: $x_4(0)$. Similarly, the trivial equilibrium’s are also replot-

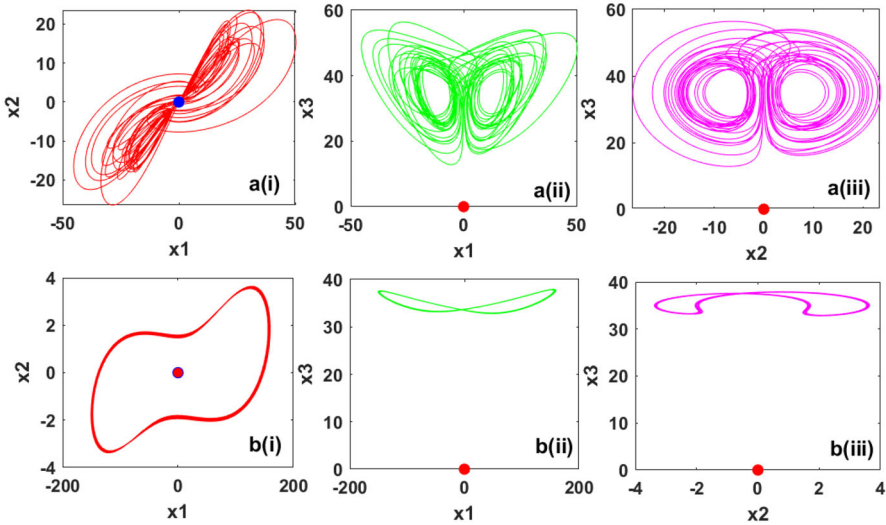


Fig. 5 Multistability: Different projections of (a) chaotic attractor (hidden) at $x_4(0) = 2.0$ and (b) periodic attractor at $x_4(0) = 20.0$. The trivial equilibrium point S_0 mentioned as blue and red dot. The other ICs: $x_1(0), x_2(0), x_3(0)$ are $(0.1, 0.1, 0)$

ted in Figure S0. Figure 5 shows the confirmation of the multistability of the hidden attractor with respect to the initial condition $x_4(0)$. By changing the initial conditions the system exhibits different behaviour as shown in Figures 5(a) chaotic and 5(b) periodic oscillation at different $x_4(0)$. The other parameters are fixed and initial conditions $(x_1(0), x_2(0), x_3(0))$ are $(0.1, 0.1, 0.0)$. The trivial equilibrium point S_0 is also replotted as a blue and red dot in Figure 5. Further, we could get a variety of attractors when the other initial conditions are varied.

3.2 Construction of fractional order memristor system

The memristive hyperchaotic system (17) constructs the fractional system using the RL fractional derivative of (11). The mathematical equations for the fractional order-based memristive hyperchaotic system is as follows:

$$\begin{cases} \frac{dx_1^{q_1}}{dt^{q_1}} = W(x_4)x_2 - \eta x_1, \\ \frac{dx_2^{q_2}}{dt^{q_2}} = \gamma x_1 - x_1 x_3 + \mu, \\ \frac{dx_3^{q_3}}{dt^{q_3}} = x_1 x_2 - \zeta x_3, \\ \frac{dx_4^{q_4}}{dt^{q_4}} = x_2. \end{cases} \tag{18}$$

Here, $q_1, q_2, q_3,$ and q_4 are fractional orders of the state variables $x_1, x_2, x_3,$ and x_4 respectively. The main aim is to find the least nonlinearity strength that exhibits chaotic oscillations in the system (18). Here, q_4 represents the fractional nonlinearity strength.

Table 1 The experimental circuit component names and values are listed in accordance with the normalisation parameters specified in the numerical section

Component name	Values
C_1, C_2, C_3, C_w	100 μF
R_x, R_y, R_z	350 $\text{k}\Omega$, 1.09 $\text{k}\Omega$, 8.75 $\text{k}\Omega$
R_2, R_3, R	10 $\text{k}\Omega$
R_4, R_6	17.5 $\text{k}\Omega$
R_5, R_7	7 $\text{M}\Omega$, 116.7 $\text{k}\Omega$
Fractional sub circuit	For $q_4 = 0.7$
C_A, C_B, C_C	0.76 μF , 0.52 μF , 1.1 μF
R_a, R_b, R_c	1.5 $\text{M}\Omega$, 6 $\text{M}\Omega$, 2.2 $\text{k}\Omega$

We fixed $q_1, q_2, q_3 = 1$, and $q_4 < 1$ to determine the fractional rate of change of flux or charge, defining the nonlinearity of the memristor.

In the experiments, we constructed the appropriate analogue circuit of our system (18) as shown in Figure 2(a). The system enforces four state variables using four integrators. The operational amplifier OP071P performs addition, subtraction, and integration. Figure 2(b) shows how the multiplier IC AD633JN controls the memristor nonlinear function. The memristor component employs the tree shape model of the fractional order operator circuit (Figure 2(c)) instead of the ‘fractional order’ represented in Figure 2(b), which displays the replacement of the capacitor C_w with a red dashed line. The dual voltage power supply provides external biasing ($\pm 1\text{V}$) based on the system physical condition. The relevant circuit parameters are established in accordance with the numerical parameters listed above. Table 1 shows the values of the components and subcircuit fractional order tree-shaped circuit components. The gains of two multipliers (M_1 and M_2) are set to one within the system (18). The elements have been carefully chosen within $\pm 1\%$ tolerance.

4 Numerical and experimental results

To compute the fractional order system (18), we used fractional forward Euler’s Method for the RL fractional derivative. Figure 6 shows the one-parameter bifurcation diagram with fractional order q_4 in ranges $q_4 \in (1.0, 0.4)$ of system (18). This bifurcation produces chaotic oscillations up to the fractional order of $q_4 = 0.4$, which exceeds the parameter value; the chaotic nature is no longer present, and the system stays in a boundary condition. It is important to remember that in this case, the chaotic oscillations are the hidden oscillations.

Nonetheless, the bifurcation diagram shows many dynamical behaviours. For another set of parameter values, we could foresee the period doubling scenario. From $q_4 \in (0.4, 0.55)$, the chaotic oscillations increase denser and widen their basin with respect to the fractional order q_4 . Figure 7 depicts phase portraits for various projections of $q_4 = 0.95$ and $q_4 = 0.4$. These two comparisons demonstrate that the size of

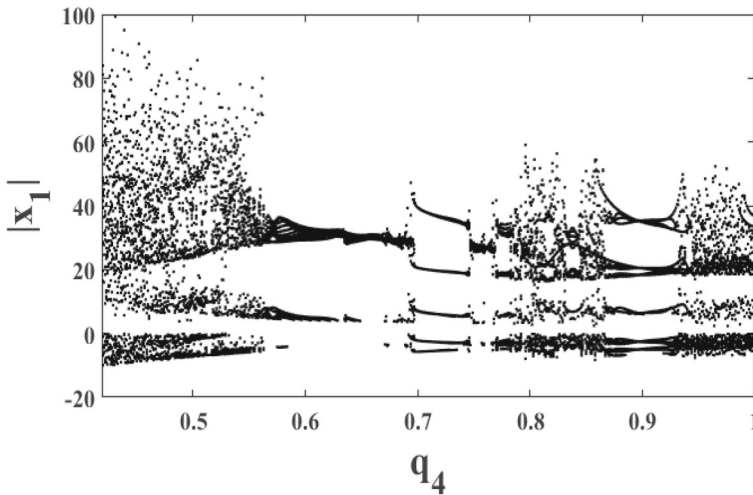


Fig. 6 One parameter bifurcation diagram of the $(q_4 - |x_1|)$ plane for the system (18). $|x_1|$ represents the maxima of variable x_1

the chaotic attractor increases as it approaches the border. The remaining fractional orders in system (18) are set at $q_1, q_2, q_3=1.0$.

To confirm the least fractional order nonlinearity chaotic attractor in experiments, the ladder network subcircuit of Figure 2(c) is constructed. For attain $q_4 = 0.7$ the first two layer of RC ladder is used. The RC ladder network further extended depends on the fractional derivative values (See tree shape model in [53]). For instance the resistance R_a, R_b, R_c and the capacitance C_1, C_2, C_3 is fixed in Table 1 for $q_4 = 0.7$ of the circuit. The rest of the circuit parameters are fixed as per the text in experimental circuit confirmations which is given in Table 1.

Figure 8 shows phase portraits and time series for the least order of nonlinearity at $q_4 = 0.4$, which produces chaotic oscillations. Chaotic oscillations do not occur above fractional order levels. Furthermore, reducing the order of q_4 increases the volume of the chaotic attractor, causing it to intersect the boundary at $q_4 = 0.4$. These experiments show that the numerical results are compatible with the results of the experiment. The data was collected from the real-time circuit via the Agilent data acquisition card at a rate of 2 GSa/s and processed in MATLAB.

4.1 Multistability

This section defines and clarifies the multistability behaviour in the fractional order system (18). Figure 9 shows the bifurcation plot between the initial condition $x_4(0)$ and the maximum of the state variable $x_2(t)$. The initial condition of $x_4(0)$, which corresponds to the flow of the memristor, changed along the range of $x_4(0) \in (-1, 1)$. The multistability can also be identified by changing the other initial conditions such as $x_1(0), x_2(0)$, and $x_3(0)$. However, for the purpose of clarity, we will not include such plots here.

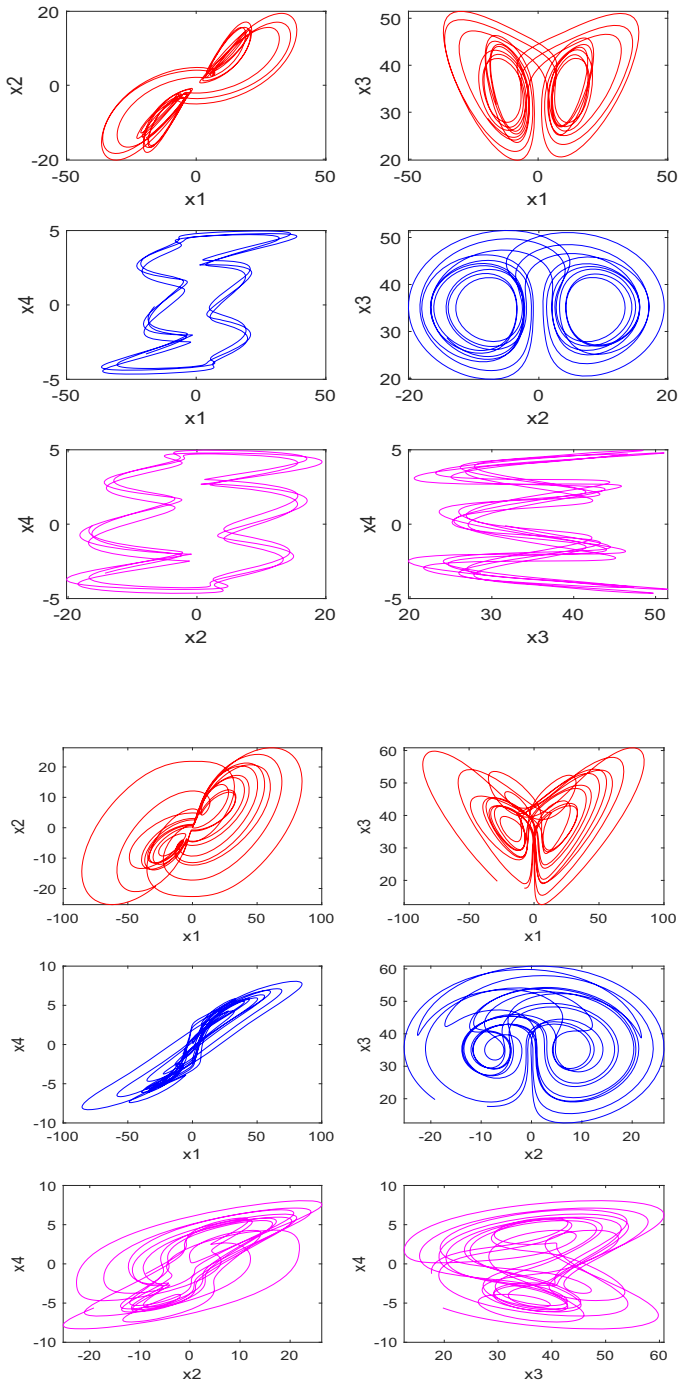


Fig. 7 Numerical computation of phase portraits in the different projections of chaotic oscillations. (upper panel) chaotic oscillation at $q_4 = 0.95$ and (lower panel) at $q_4 = 0.4$

Fig. 8 Least fractional order: (a) numerical and (b) experimental observations of the different projections of phase portrait (i) $x_1 - x_2$ and (iii) $x_2 - x_3$ planes and the corresponding time series of (ii) x_1 and (iv) x_2 variables, respectively, by fixing $q_4 = 0.4$

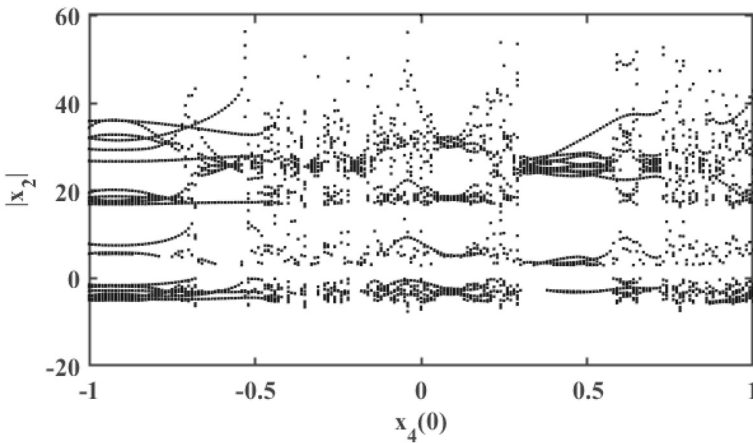
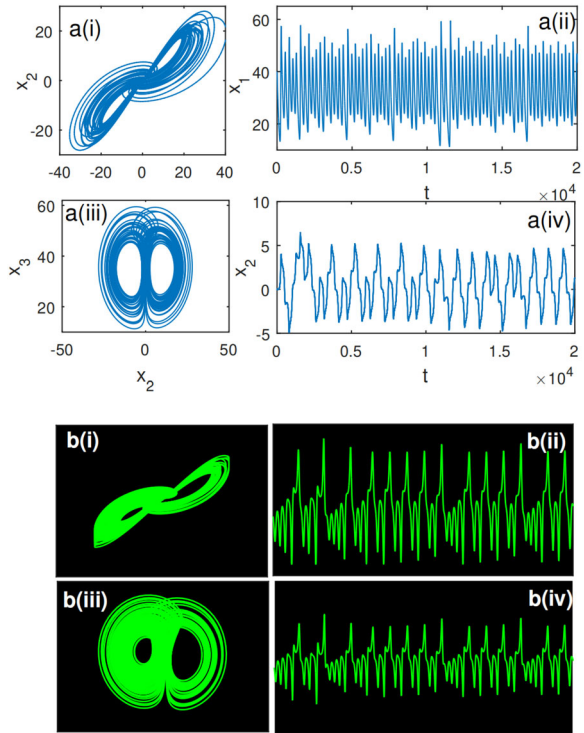


Fig. 9 One parameter bifurcation diagram in $(x_4(0) - |x_2|)$ plane of system (18). $|x_2|$ denotes maxima of state variable x_2

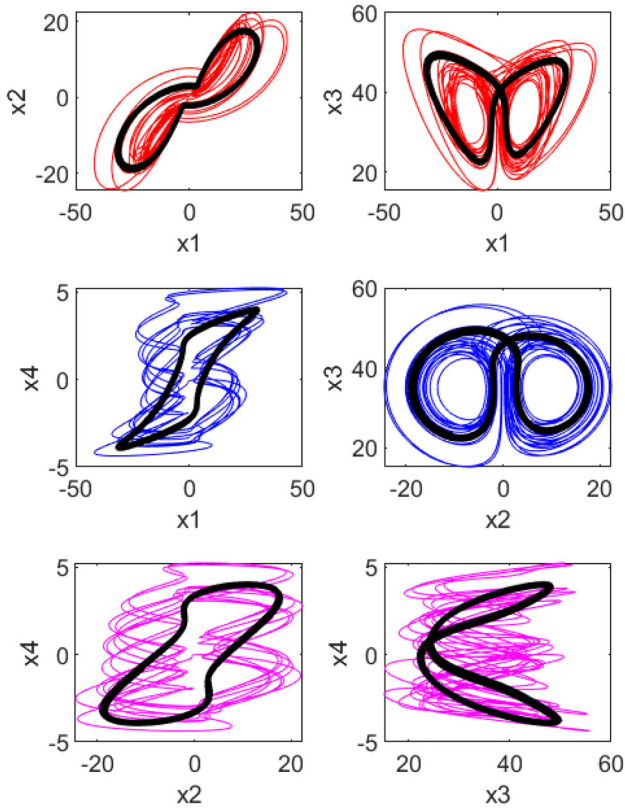


Fig. 10 Numerical observations of various phase portrait projections. The periodic attractors obtained at $x_4(0) = 0.4$ are represented in the block line through the chaotic oscillation at $x_4(0) = 0.9$

The bifurcation plot depicts both periodic and chaotic regimes. The system parameters and fractional orders are fixed, but the initial conditions only vary. The bifurcation diagram demonstrates multistability.

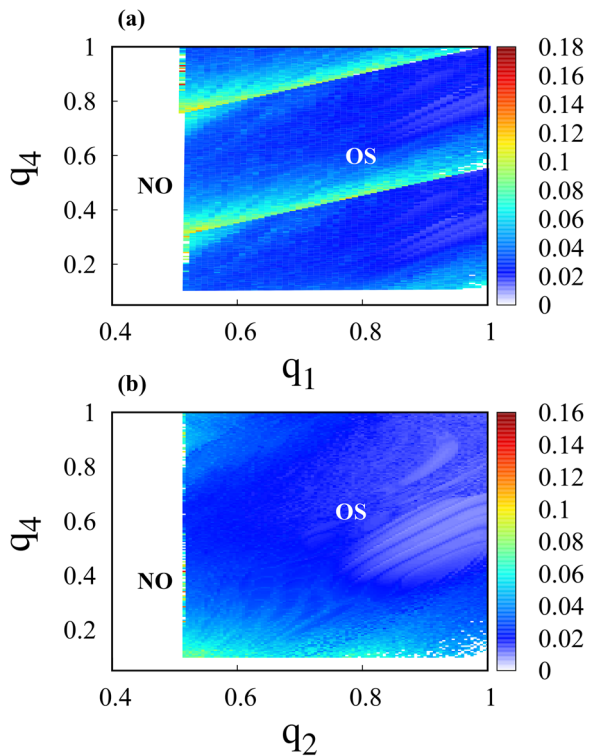
Figure 10 depicts the phase portraits from different projections for better understanding. The chaotic attractor is shown with different colours, and the periodic attractors are mentioned in the black line on the chaotic attractor for the sake of demonstration.

4.2 Two parameter scanning

Two-parameter scanning is used to identify the limit of basin’s oscillation regime in order to acquire a global understanding. Figure 11(a,b) depicts a two-parameter scanning plot that shows how the fractional nonlinearity q_4 varies in relation to the other fractional state variables q_1 and q_2 .

The frequency of the oscillation is computed and it is mentioned in colour bar. The nonzero frequency regions of the two-parameter scanning plots identify the oscillatory

Fig. 11 Two parameters of the system (18) are scanned: (a) q_1 vs q_4 fractional order plane and (b) q_2 versus q_4 fractional order plane. The numerical frequency is calculated to separate chaotic and boundary motions



portions, while the zeroth frequency portions identify the non-oscillatory portions. The oscillatory portion, named (OS) is mentioned in the coloured region. The white colour symbolises the system absence of oscillation, named (NO). This basin plot highlighted the global dynamical features as well as the lowest order of functioning. However, this two-parameter plot shows the presence of a ‘multistability’ phenomenon in the suggested system (18). In addition, a third fractional order variable scan is performed. It is avoided here in order to maintain things simple.

5 Conclusions

The least fractional nonlinearity for showing chaos in a memristor-based hyper-chaotic multistable hidden system is studied. The nonlinearity dimension varied fractionally, and the minimal order of nonlinearity required to generate chaos in our proposed system is identified. Furthermore, the multistability of the systems is thoroughly studied, and the hidden attractors are investigated in several projections with interpretations. The proposed system global dynamics can be better understood by employing the two-parameter frequency scanning method. This study examines the system dynamics through analytical, numerical, and experimental methods.

Acknowledgements SS & VP acknowledge the Basic Research Program of the National Research University, Higher School of Economics, Moscow.

Author contributions All authors contributed equally and significantly to writing this manuscript and typed, read, and approved the final manuscript.

Declarations

Competing interests The authors declare that they have no competing interests.

References

1. Adamatzky, A., Chua, L.: *Memristor Networks*. Springer Science & Business Media (2013)
2. Ahmad, W.M., Sprott, J.C.: Chaos in fractional-order autonomous nonlinear systems. *Chaos, Solitons & Fractals* **16**(2), 339–351 (2003)
3. Azar, A.T., Vaidyanathan, S., Ouannas, A.: *Fractional Order Control and Synchronization of Chaotic Systems*. Springer (2017)
4. Bakkyaraj, T., Sahadevan, R.: Invariant analysis of nonlinear fractional ordinary differential equations with Riemann-Liouville fractional derivative. *Nonlinear Dynamics* **80**, 447–455 (2015)
5. Bao, B., Bao, H., Wang, N., Chen, M., Xu, Q.: Hidden extreme multistability in memristive hyperchaotic system. *Chaos, Solitons & Fractals* **94**, 102–111 (2017)
6. Caputo, M.: Linear models of dissipation whose q is almost frequency independent-ii. *Geophysical Journal International* **13**(5), 529–539 (1967)
7. Chang, H., Li, Y., Yuan, F., Chen, G.: Extreme multistability with hidden attractors in a simplest memristor-based circuit. *International Journal of Bifurcation and Chaos* **29**(06), 1950086 (2019)
8. Chen, M., Li, M., Yu, Q., Bao, B., Xu, Q., Wang, J.: Dynamics of self-excited attractors and hidden attractors in generalized memristor-based Chua's circuit. *Nonlinear Dynamics* **81**(1), 215–226 (2015)
9. Chen, Y., Cao, Q., Zhu, Z., Wang, Z., Zhao, Z.: Switched fuzzy sampled-data control of chaotic systems with input constraints. *IEEE Access* **9**, 44402–44410 (2021)
10. Chua, L.: Memristor-the missing circuit element. *IEEE Transactions on Circuit Theory* **18**(5), 507–519 (1971)
11. Diethelm, K., Ford, N.: *The Analysis of Fractional Differential Equations*. Lecture Notes in Mathematics **2004** (2010)
12. Duan, B., Zheng, Z., Cao, W.: Spectral approximation methods and error estimates for Caputo fractional derivative with applications to initial-value problems. *Journal of Computational Physics* **319**, 108–128 (2016)
13. Ge, Z.M., Ou, C.Y.: Chaos in a fractional order modified Duffing system. *Chaos, Solitons & Fractals* **34**(2), 262–291 (2007)
14. Grigorenko, I., Grigorenko, E.: Chaotic dynamics of the fractional Lorenz system. *Physical Review Letters* **91**(3), 034101 (2003)
15. Jafari, S., Ahmadi, A., Khalaf, A.J.M., Abdolmohammadi, H.R., Pham, V.T., Alsaadi, F.E.: A new hidden chaotic attractor with extreme multi-stability. *AEU-International Journal of Electronics and Communications* **89**, 131–135 (2018)
16. Ji'e, M., Yan, D., Wang, L., Duan, S.: Hidden attractor and multistability in a novel memristor-based system without symmetry. *International Journal of Bifurcation and Chaos* **31**(11), 2150168 (2021)
17. Kozma, R., Pino, R.E., Paziienza, G.E.: *Advances in Neuromorphic Memristor Science and Applications*. Springer Science & Business Media (2012)
18. Latifzadeh, H.: A coupling method of homotopy technique and laplace transform for nonlinear fractional differential equations. *International Journal of Advances in Applied Sciences* **1**(4), 159–170 (2012)
19. Leonov, G.A., Kuznetsov, N.V.: Hidden attractors in dynamical systems. From hidden oscillations in Hilbert–Kolmogorov, Aizerman, and Kalman problems to hidden chaotic attractor in Chua circuits. *International Journal of Bifurcation and Chaos* **23**(01), 1330002 (2013)
20. Li, C., Liao, X., Yu, J.: Synchronization of fractional order chaotic systems. *Physical Review E* **68**(6), 067203 (2003)

21. Lin, Z., Wang, H.: Efficient image encryption using a chaos-based PWL memristor. *IETE Technical Review* **27**(4), 318–325 (2010)
22. Magin, R.L.: Fractional calculus in bioengineering, part 1. *Critical Reviews in Biomedical Engineering* **32**(1), 1 (2004)
23. Muñoz-Pacheco, J.M.: Infinitely many hidden attractors in a new fractional-order chaotic system based on a fracmemristor. *The European Physical Journal Special Topics* **228**(10), 2185–2196 (2019)
24. Muthuswamy, B.: Implementing memristor based chaotic circuits. *International Journal of Bifurcation and Chaos* **20**(05), 1335–1350 (2010)
25. Oldham, K., Spanier, J.: *The Fractional Calculus Theory and Applications of Differentiation and Integration to Arbitrary Order*. Elsevier (1974)
26. Palanivel, J., Suresh, K., Sabarathinam, S., Thamilmaran, K.: Chaos in a low dimensional fractional order nonautonomous nonlinear oscillator. *Chaos, Solitons & Fractals* **95**, 33–41 (2017)
27. Petráš, I.: Fractional-order chaotic systems. In: *Fractional-order nonlinear systems*, pp. 103–184. Springer (2011)
28. Petráš, I.: *Fractional-order Nonlinear Systems: Modeling, Analysis and Simulation*. Springer Science & Business Media (2011)
29. Pham, V.T., Volos, C., Kapitaniak, T.: *Systems with Hidden Attractors: From Theory to Realization in Circuits*. Springer (2017)
30. Pham, V.T., Volos, C.K., Vaidyanathan, S., Le, T., Vu, V.: A memristor-based hyperchaotic system with hidden attractors: Dynamics, synchronization and circuitual emulating. *Journal of Engineering Science & Technology Review* **8**(2) (2015)
31. Prakash, P., Singh, J.P., Roy, B.: Fractional-order memristor-based chaotic jerk system with no equilibrium point and its fractional-order backstepping control. *IFAC-PapersOnLine* **51**(1), 1–6 (2018)
32. Rogosin, S., Karpinyenya, M.: Fractional models for analysis of economic risks. *Fractional Calculus and Applied Analysis* **26**(6), 2602–2617 (2023)
33. Sabarathinam, S., Prasad, A.: Memristor emulator causes dissimilarity on a coupled memristive systems. In: *AIP Conference Proceedings*, vol. 1942, p. 060025. AIP Publishing LLC (2018)
34. Samko, S.G., Kilbas, A.A., Marichev, O.O.: *Fractional Integrals and Derivatives (Theory and Applications)*. Gordon and Breach, Switzerland (1993)
35. Sengupta, A.: *Chaos, Nonlinearity, Complexity: The Dynamical Paradigm of Nature*. Springer (2006)
36. Sharma, P.K., Ranjan, R.K., Khateb, F., Kumngern, M.: Charged controlled mem-element emulator and its application in a chaotic system. *IEEE Access* **8**, 171397–171407 (2020)
37. Strukov, D.B., Snider, G.S., Stewart, D.R., Williams, R.S.: The missing memristor found. *Nature* **453**(7191), 80–83 (2008)
38. Sun, H., Jiang, Y., Zhang, Y., Jiang, L.: A review of constitutive models for non-Newtonian fluids. *Fractional Calculus and Applied Analysis* **27**(4), 1483–1526 (2024). <https://doi.org/10.1007/s13540-024-00294-0>
39. Tavazoei, M.S.: Fractional order chaotic systems: history, achievements, applications, and future challenges. *The European Physical Journal Special Topics* **229**(6), 887–904 (2020)
40. Tetzlaff, R.: *Memristors and Memristive Systems*. Springer (2013)
41. Trujillo, J., Rivero, M., Bonilla, B.: On a Riemann-Liouville generalized Taylor's formula. *Journal of Mathematical Analysis and Applications* **231**(1), 255–265 (1999)
42. Varshney, V., Sabarathinam, S., Prasad, A., Thamilmaran, K.: Infinite number of hidden attractors in memristor-based autonomous duffing oscillator. *International Journal of Bifurcation and Chaos* **28**(01), 1850013 (2018)
43. Varshney, V., Sabarathinam, S., Prasad, A., Thamilmaran, K.: Infinite number of hidden attractors in memristor-based autonomous duffing oscillator. *International Journal of Bifurcation and Chaos* **28**(01), 1850013 (2018)
44. Vinagre, B., Podlubny, I., Hernandez, A., Feliu, V.: Some approximations of fractional order operators used in control theory and applications. *Fractional Calculus and Applied Analysis* **3**(3), 231–248 (2000)
45. Wang, M., Deng, B., Peng, Y., Deng, M., Zhang, Y.: Hidden dynamics, synchronization, and circuit implementation of a fractional-order memristor-based chaotic system. *The European Physical Journal Special Topics* **231**(16), 3171–3185 (2022)
46. Wang, N., Zhang, G., Kuznetsov, N.V., Bao, H.: Hidden attractors and multistability in a modified chua's circuit. *Communications in Nonlinear Science and Numerical Simulation* **92**, 105494 (2021)

47. Wang, N., Zhang, G., Kuznetsov, N.V., Li, H.: Generating grid chaotic sea from system without equilibrium point. *Communications in Nonlinear Science and Numerical Simulation* **107**, 106194 (2022)
48. Wang, X., Kuznetsov, N.V., Chen, G.: *Chaotic Systems with Multistability and Hidden Attractors*. Springer (2021)
49. Wang, Z., Liu, J., Zhang, F., Leng, S.: Hidden chaotic attractors and synchronization for a new fractional-order chaotic system. *Journal of Computational and Nonlinear Dynamics* **14**(8), 081010 (2019)
50. Williams, R.S.: How we found the missing memristor. *IEEE Spectrum* **45**(12), 28–35 (2008)
51. Wu, H., Ye, Y., Bao, B., Chen, M., Xu, Q.: Memristor initial boosting behaviors in a two-memristor-based hyperchaotic system. *Chaos, Solitons & Fractals* **121**, 178–185 (2019)
52. Xiang-Rong, C., Chong-Xin, L., Fa-Qiang, W.: Circuit realization of the fractional-order unified chaotic system. *Chinese Physics B* **17**(5), 1664 (2008)
53. Xiang-Rong, C., Chong-Xin, L., Fa-Qiang, W.: Circuit realization of the fractional-order unified chaotic system. *Chinese Physics B* **17**(5), 1664 (2008)
54. Xu, Q., Lin, Y., Bao, B., Chen, M.: Multiple attractors in a non-ideal active voltage-controlled memristor based chua's circuit. *Chaos, Solitons & Fractals* **83**, 186–200 (2016)

Publisher's Note Springer Nature remains neutral with regard to jurisdictional claims in published maps and institutional affiliations.

Springer Nature or its licensor (e.g. a society or other partner) holds exclusive rights to this article under a publishing agreement with the author(s) or other rightsholder(s); author self-archiving of the accepted manuscript version of this article is solely governed by the terms of such publishing agreement and applicable law.